



Blood Memory Color Reproduction for Endoscopic Images

Xingkun He^{1,2,*}, Shi Yang²

¹Shenzhen Institutes of Advanced Technology, Chinese Academy of Sciences, Shenzhen 518000, Guangdong, China.

²Shenzhen Mindray Bio-Medical Electronics Co., Ltd., Shenzhen 518000, Guangdong, China.

How to cite this paper: Xingkun He, Shi Yang. (2026) Blood Memory Color Reproduction for Endoscopic Images. *Advances in Computer and Communication*, 7(1), 14-21. DOI: 10.26855/acc.2026.03.003

Received: December 31, 2025

Accepted: January 29, 2026

Published: February 28, 2026

***Corresponding author:** Xingkun He, Shenzhen Institutes of Advanced Technology, Chinese Academy of Sciences, Shenzhen 518000, Guangdong, China; Shenzhen Mindray Bio-Medical Electronics Co., Ltd., Shenzhen 518000, Guangdong, China.

Abstract

This study presents a specialized memory-color-based algorithm specifically designed to achieve accurate blood color reproduction in endoscopic imaging. The algorithmic development commenced with a series of psychophysical experiments aimed at quantitatively determining the optimal target coordinates for blood memory color within the HSV (Hue, Saturation, Value) color space. Based on these findings, a dedicated blood color reproduction framework was constructed, which systematically incorporates three core modules: blood color detection, memory color center definition, and memory color adjustment. The superior performance of the proposed method in reproducing realistic blood color was comprehensively validated through extensive comparative experiments conducted on multiple diverse sets of endoscopic images. Furthermore, a psychophysical evaluation involving a panel of four clinically trained observers was performed to assess subjective visual quality. The results demonstrated a 100% preference rate for the images reproduced by the proposed method compared to the original images, confirming its potential effectiveness for clinical applications.

Keywords

Blood memory color; Color reproduction; Endoscopic image processing; Psychophysical experiment

1. Introduction

Endoscopy is a diagnostic and therapeutic modality that enables direct visualization and intervention within body cavities through natural orifices or minimal access points [1-3]. Characterized by minimal invasiveness, real-time imaging, and high diagnostic accuracy, endoscopy has been established as an indispensable technology in modern minimally invasive surgery. Endoscopic imaging systems are based on optical propagation and image sensor technology, enabling real-time visualization of internal tissues in patients. However, due to disparities in spectral response between image sensors and the human eye [4], as well as the multiple reflections of the illumination light [5], endoscopic images exhibit color deviations from reality, impairing physicians' ability to identify pathological tissues [6]. Consequently, the accurate reproduction of colors in endoscopic images has been a primary area of research focus.

In recent years, scholars both domestically and internationally have conducted extensive research on color correction in endoscopic images. For instance, to enhance the color accuracy of endoscopic images, Chen et al. proposed a color correction algorithm based on four-neighborhood polynomial regression [7]. To adapt color correction methods to non-uniform illumination conditions in endoscopy, Wang et al. introduced a dynamic CCM (Color Correction Matrix) method based on image brightness [8]. Furthermore, Cheng developed an endoscopic color correction assessment methodology based on the CIELAB color space [9]. This method evaluates the color discriminability and fidelity of endoscopic images captured from color charts, enabling quantitative assessment of endoscopic image color

performance. The aforementioned studies have advanced the development of color correction in endoscopic imaging, yet they have overlooked the influence of memory colors on endoscopic color correction.

Memory color representations for frequently encountered objects have been demonstrated in the human visual system [10-12]. For instance, the formation of traditional memory colors such as skin tones, foliage green, and sky blue relies on their high frequency and chromatic stability in natural environments [13-15]. The color of blood is primarily determined by three physiological parameters: hematocrit, hemoglobin concentration, and oxygen saturation [16]. Furthermore, Mo et al. demonstrated that porcine blood within normal physiological ranges exhibits similar hematocrit and hemoglobin concentrations to human blood [17]. Chang et al. confirmed that the color difference of arterial porcine blood under normal physiological conditions is minimal [18]. Collectively, these studies demonstrate the stability of human blood color characteristics. In surgical settings, the chromatic stability and high frequency of blood support its recognition as a memory color for surgeons.

In this paper, a memory-color-based method for blood color reproduction is proposed. The center of the blood memory color is determined through psychophysical experiments. The blood color in endoscopic images is adjusted toward the memory color by modifying two color dimensions: hue and saturation. To the best of our knowledge, the application of blood memory color in endoscopic image color reproduction has not been previously studied. Experimental results demonstrate that the proposed method achieves excellent blood color reproduction performance. In this study, blood memory color refers specifically to the perceptual prototype derived from observer preference rather than long-term semantic memory.

2. Experiment

2.1 Images and display color characterization

In real-time image signal processing, the HSV (Hue, Saturation, Value) color space is more frequently utilized than the CIELAB color space. Consequently, this study employs the HSV color model with the BT.2020 (Broadcast Service Television 2020) color gamut to characterize blood color [19, 20]. As shown in Figure 1, a total of 400 HSV combinations are used to simulate different blood colors. The 400 samples were uniformly distributed in the H-S plane with fixed $V = 0.35$ to isolate chromatic effects. The resulting HSV colors are subsequently converted into the RGB color space and then subjected to the Opto-Electronic Transfer Function to generate images ready for display, as illustrated in Equation (1).

$$\begin{aligned} H_w &= 0 + H & H &\in [0, 0.02] \\ S_w &= 0.6 + S & S &\in [0, 0.4] \\ V_w &= 0.35 \end{aligned} \quad (1)$$

The experiment is conducted using a Sony LMD-XH320T medical monitor, which has a 32-inch LCD display with a resolution of 3840×2160 pixels and BT.2020 color gamut. Moreover, the color consistency of the display is assessed to be acceptable, with a mean difference of $1.5 \Delta E_{00}$ units.

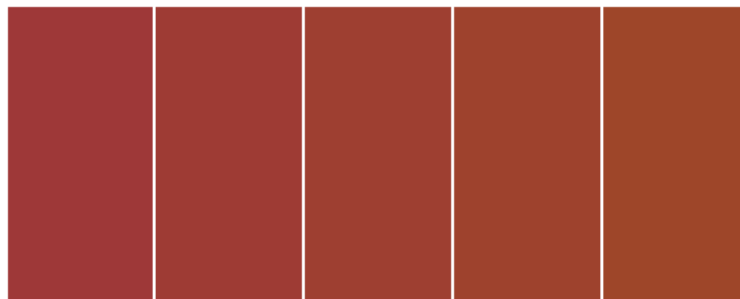


Figure 1. Simulated images of blood color.

2.2 Experimental procedure

The experiment was conducted in a bright room with a lighting color temperature of 6500 K. The display was positioned at the center of the room, one meter away from the observer, to simulate the scenario of a minimally invasive surgery room. The experimental setup is illustrated in Figure 2.

Four observers participated in the experiment. All observers had a clinical medicine education background and passed the Ishihara color vision test. Prior to the formal experiment, the research team explained the procedure to the

observers. Each observer then evaluated five practice images to familiarize themselves with the process. During the formal experiment, each observer assessed 400 simulated blood images. The images were presented individually in a random sequence; after an observer categorized an image as "Like" or "Dislike," the next image was displayed.



Figure 2. Schematic of the experimental environment simulating a minimally invasive surgery room.

2.3 Data analysis

Inter-observer variation refers to the deviation between each observer's experimental results and the average results of all observers. This study quantified the inter-observer variation using the MCDM (Mean Color Difference from the Mean), as shown in Equation (2).

$$MCDM = \frac{\sum_{i=1}^n \Delta HS_i}{n} \tag{2}$$

and

$$\begin{aligned} \Delta HS_i &= \sqrt{(H_i - H_m)^2 + (S_i - S_m)^2} \\ H_m &= \frac{\sum_{i=1}^n H_i}{n} \\ S_m &= \frac{\sum_{i=1}^n S_i}{n} \end{aligned} \tag{3}$$

where n is the number of observers, H_i and S_i are the average blood memory color coordinates for each observer, and H_m and S_m are the average blood memory color coordinates for all observers. A smaller MCDM value indicates lower variability. Furthermore, the MCDM can also be applied to describe intra-observer variation.

The average MCDM for inter-observer variation was 0.015, while the average MCDM for intra-observer variation was 0.01, indicating relatively high consistency both within and between observers. Figure 3 displays the blood memory colors and their tolerance ellipses selected by four observers. Based on these results, the values $H=0.01$ and $S=0.93$ were established as the endoscopic blood memory color.

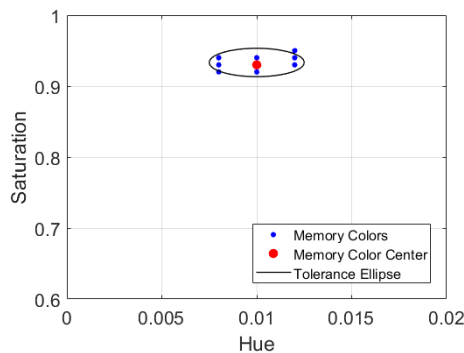


Figure 3. Distribution of endoscopic blood memory colors in Hue-Saturation space.

3. Methods

Due to variations in the spectral transmittance of different endoscopes and the influence of ambient light, the color of blood in endoscope images may undergo changes. Therefore, this paper proposes the blood memory color reproduction algorithm for endoscopic images, which can be divided into three components: blood color detection, memory blood color definition, and blood color reproduction, as illustrated in Figure 4.

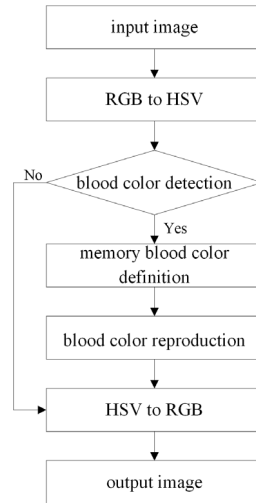


Figure 4. The flow of blood memory color reproduction algorithm.

3.1 Blood color detection

RGB, CIELAB, and HSV color spaces are commonly used for memory color detection. However, endoscopes utilize LED light sources for illumination, which possess point-source characteristics, resulting in uneven brightness in endoscopic images. Consequently, the variation range of blood brightness is also extensive. Considering that the hue and saturation in the HSV color space are independent of luminance changes, this paper adopts HSV as the color space for blood color detection.

An analysis of the color characteristics of endoscopic images from various surgical procedures indicates that blood exhibits a higher color saturation than fat, mucosa, organs, and other tissues, presenting a unique chromatic feature. Moreover, the actual color of blood is influenced by key physiological parameters (e.g., hemoglobin concentration, oxygen saturation, and red blood cell concentration), which lead to subtle color variations across different anatomical regions. Therefore, this paper employs the distribution patterns of hue and saturation for blood color detection. As shown in Equation (4), the range of blood colors corresponds to a rectangular region within the hue-saturation color space.

$$\begin{cases} 0.002 + k_1 < H < 0.018 + k_2 \\ 0.75 + k_3 < S < 1 + k_4 \\ 0.05 + k_5 < V < 1 + k_6 \end{cases} \quad (4)$$

where k_1, k_2, k_3, k_4, k_5 and k_6 are empirical coefficients used to adjust the range of blood color detection.

3.2 Memory blood color definition

According to the psychophysical experiment results presented in Section 2.3, $H=0.01$ and $S=0.93$ can be regarded as the central value of the memory color for blood. Therefore, the proposed blood memory color reproduction algorithm defines the effective blood memory color as $H=0.01$ and $S=0.93$.

3.3 Blood color reproduction

The approximate model representing the blood memory color and the detected blood color distribution range in endoscopic images is illustrated in the HS color plane in Figure 5.

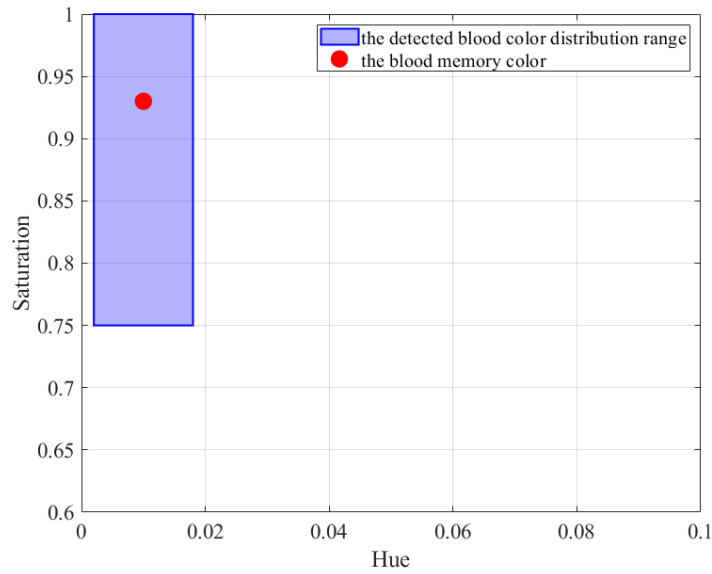


Figure 5. The distribution of blood color detected and blood memory color in the HS plane.

The red region denotes the blood memory color, while the blue region indicates the detected blood distribution in endoscopic images. The hue and saturation of blood in endoscopic images are adjusted toward the theoretical values of the memory color range. The adjusted hue and saturation of blood are calculated using the following formulas:

$$H_{new} = H_{ori} + \frac{(H_0 - H_1)}{2} * \sin\left(\frac{H_{ori} - H_1}{H_0 - H_1} * \pi\right), \quad H_1 < H_{ori} < H_0 \quad (5)$$

$$H_{new} = H_{ori} + \frac{(H_2 - H_0)}{2} * \sin\left(\frac{H_2 - H_{ori}}{H_2 - H_0} * \pi\right), \quad H_0 < H_{ori} < H_2 \quad (6)$$

$$S_{new} = S_{ori} + \frac{(S_0 - S_1)}{2} * \sin\left(\frac{S_{ori} - S_1}{S_0 - S_1} * \pi\right), \quad S_1 < S_{ori} < S_0 \quad (7)$$

$$S_{new} = S_{ori} + \frac{(S_2 - S_0)}{2} * \sin\left(\frac{S_2 - S_{ori}}{S_2 - S_0} * \pi\right), \quad S_0 < S_{ori} < S_2 \quad (8)$$

where H_1 , H_2 , S_1 and S_2 are detected blood color distribution range in endoscopic images, and H_0 and S_0 represent the blood memory color.

4. Validation

This section presents a comparative analysis of five paired endoscopic images before and after blood color memory reproduction, processed in the BT.2020 color space, as shown in Figure 6. In each pair, the left image represents the original result before memory color reproduction, while the right image displays the enhanced outcome after reproduction. To evaluate the performance, a psychophysical experiment was conducted in which each participant was sequentially presented with image pairs (before and after reproduction) and required to perform a forced-choice selection of the preferred alternative. The results indicate that 100% of the preferred selections corresponded to the images after blood memory color reproduction.

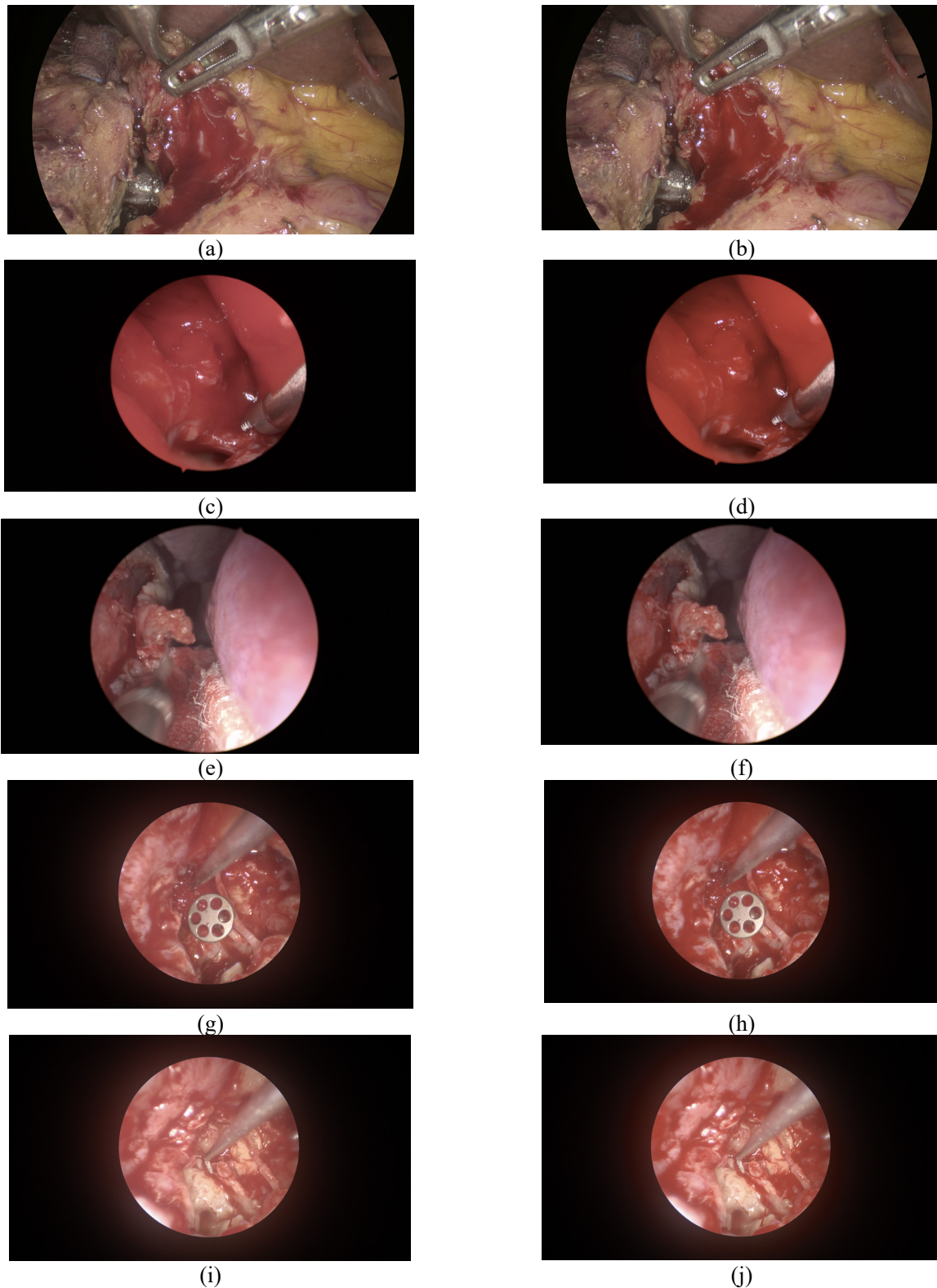


Figure 6. (a) Original laparoscopic image 1, (b) Laparoscopic image 1 after blood memory color reproduction, (c) Original nasal endoscopic image 2, (d) Nasal endoscopic image 2 after blood memory color reproduction, (e) Original nasal endoscopic image 3, (f) Nasal endoscopic image 3 after blood memory color reproduction, (g) Original otoscopic endoscopic image 4, (h) Otoscopic endoscopic image 4 after blood memory color reproduction, (i) Original otoscopic endoscopic image 5, (j) Otoscopic endoscopic image 5 after blood memory color reproduction.

5. Conclusion

This paper proposes a memory-color-based algorithm for blood color reproduction in endoscopic images. First, the memory color center for blood in the HSV color space is determined through psychophysical experiments. Then, blood region detection is accomplished based on prior knowledge of color saturation characteristics in endoscopic images. Finally, precise blood color reproduction is achieved by calculating the distance in hue and saturation between the actual blood color in the image and the predefined memory color. Experimental results demonstrate that the proposed method achieves superior blood color reproduction performance compared to the original blood color in endoscopic images. The small observer sample size and binary preference task limit statistical generalization; future studies will incorporate larger cohorts and continuous rating scales.

Conflict of Interest

All authors reviewed the manuscript and declared that there were no competing financial interests in this work.

References

- [1] Khanicheh A, Shergill AK. Endoscope design for the future. *Tech Gastrointest Endosc.* 2019;21:167-73.
- [2] Boese A, Wex C, Croner R, Liehr UB, Wendler JJ, Weigt J, et al. Endoscopic imaging technology today. *Diagnostics.* 2022;12:1262.
- [3] Alkatout I, Mechler U, Mettler L, Pape J, Maass N, Biebl M, et al. The development of laparoscopy—a historical overview. *Front Surg.* 2021;8:799442.
- [4] Toivonen ME, Klami A. Practical camera sensor spectral response and uncertainty estimation. *J Imaging.* 2020;6:79.
- [5] Kitoh S, Obi T, Yamaguchi M, Ohyama N. Compensation of color shift due to the multiple reflection of illumination in CCD endoscopic color measurement:(1) principle and basic experiment. *Opt Commun.* 1997;143:102-8.
- [6] Badano A, Revie C, Casertano A, Cheng WC, Green P, Kimpe T, et al. Consistency and standardization of color in medical imaging: a consensus report. *J Digit Imaging.* 2015;28:41-52.
- [7] Chen J, Wang LQ, Meng ZB, Yuan B, Duan HL. Color correction for high-definition electronic endoscope. *J Innov Opt Health Sci.* 2012;5:1250029.
- [8] Wang L, Li Q, Yang H, Huang J, Xu K. A sample-based color correction method for laparoscopic images. In: 2020 IEEE International Conference on Real-Time Computing and Robotics (RCAR). IEEE; 2020. p. 446-51.
- [9] Cheng WC. Color performance review (cpr): A color performance analyzer for endoscopy devices. *J Imaging Sci Technol.* 2023;67:1-9.
- [10] Bartleson CJ. Memory colors of familiar objects. *J Opt Soc Am.* 1960;50:73-7.
- [11] Liao S, Yoshizawa T. Memory colors of familiar objects induce general color preference. *Color Res Appl.* 2024;49:79-92.
- [12] Yendrikhovskij S, Blommaert F, De Ridder H. Representation of memory prototype for an object color. *Color Res Appl.* 1999;24:393-410.
- [13] Qin B, Zhu Y, Wang L, Luo MR. Impact of Lightness on the Preferred Center of Skin Color. In: China Academic Conference on Printing and Packaging. Springer; 2024. p. 9-20.
- [14] Peng R, Luo MR, Zhu Y, Liu X, Pointer M. Preferred skin reproduction of different skin groups. *Vision Res.* 2023;207:108210.
- [15] Luo MR. The new preferred memory color (PMC) chart. *Color Res Appl.* 2024;49:564-76.
- [16] Bosschaart N, Edelman GJ, Aalders MC, van Leeuwen TG, Faber DJ. A literature review and novel theoretical approach on the optical properties of whole blood. *Lasers Med Sci.* 2014;29:453-79.
- [17] Mo J, Lu Y, Xing T, Xu D, Zhang K, Zhang S, et al. Blood metabolic and physiological profiles of Bama miniature

- pigs at different growth stages. *Porcine Health Manag.* 2022;8:35.
- [18] Chang H, Kim YL, Hassan A, Fitzgerald PJ. Whole blood reflectance for assessment of hematologic condition and detection of angiographic contrast media. *Appl Opt.* 2009;48:2435-43.
- [19] Schwarz MW, Cowan WB, Beatty JC. An experimental comparison of RGB, YIQ, LAB, HSV, and opponent color models. *ACM Trans Graph.* 1987;6:123-58.
- [20] Sugawara M, Choi SY, Wood D. Ultra-high-definition television (Rec. ITU-R BT. 2020): A generational leap in the evolution of television [standards in a nutshell]. *IEEE Signal Process Mag.* 2014;31:170-4.